Switching of α-Catenin From Epithelial to Neuronal Type During Lens Epithelial Cell Differentiation

Rupalatha Maddala[1] and Ponugoti Vasantha Rao[1,2]

[1]Department of Ophthalmology, Duke University School of Medicine, Durham, North Carolina, United States
[2]Department of Pharmacology and Cancer Biology, Duke University School of Medicine, Durham, North Carolina, United States

Correspondence: Ponugoti Vasantha Rao, Duke Eye Center, 2351 Erwin Road, Durham, NC 27710, USA; p.rao@dm.duke.edu.

Submitted: January 23, 2017
Accepted: June 6, 2017

Citation: Maddala R, Rao PV. Switching of α-catenin from epithelial to neuronal type during lens epithelial cell differentiation. *Invest Ophthalmol Vis Sci*. 2017;58:3445–3455. DOI: 10.1167/iovs.17-21539

Purpose. Ocular lens fiber cell elongation, differentiation, and compaction are associated with extensive reorganization of cell adhesive interactions and cytoskeleton; however, our knowledge of proteins critical to these events is still evolving. This study characterizes the distribution pattern of neuronal-specific α-catenin (αN-catenin) and its interaction with the N-cadherin–associated adherens junctions (AJs) and their stability in the mouse lens fibers.

Methods. Expression and distribution of αN-catenin in developing mouse and adult human lenses was determined by RT-PCR, immunoblot, and immunofluorescence analyses. Characterization of αN-catenin and N-cadherin interacting proteins and colocalization analyses were performed using immunoprecipitation, mass spectrometry, and confocal imaging. Effects of periaxin deficiency on the stability of lens fiber cell AJs were evaluated using perixin-null mice.

Results. αN-catenin exhibits discrete distribution to lens fibers in both mouse and human lenses, undergoing a robust up-regulation during fiber cell differentiation and maturation. Epithelial-specific α-catenin (αE-catenin), in contrast, distributes primarily to the lens epithelium. αN-catenin and N-cadherin reciprocally coimmunoprecipitate and colocalize along with β-catenin, actin, spectrin, vinculin, Armadillo repeat protein deleted in velo-cardio-facial syndrome homolog, periaxin, and ankyrin-B in lens fibers. Fiber cells from periaxin-null mouse lenses revealed disrupted N-cadherin/αN-catenin–based AJs.

Conclusions. These results suggest that the discrete shift in α-catenin expression from αE-catenin to αN-catenin subtype that occurs during lens epithelial cell differentiation may play a key role in fiber cell cytoarchitecture by regulating the assembly and stability of N-cadherin–based AJs. This study also provides evidence for the importance of the fiber cell–specific cytoskeletal interacting periaxin, in the stability of N-cadherin/αN-catenin–based AJs in lens fibers.

Keywords: lens, differentiation, α-catenins, adherens junctions, N-cadherin, periaxin

Dynamic regulation of cell adhesive interactions plays a fundamental role in morphogenesis and maintenance of organ shape, tissue architecture, and function.[1,2] The transparent and avascular ocular lens, which plays a crucial role in vision by focusing the incident light onto the retina, is composed of epithelial cells and their differentiated and elongated cells called fibers. Fiber cells constitute the bulk of the lens.[3] During lens development, primary fibers are formed by the elongation and differentiation of epithelial cells of the posterior lens vesicle, whereas secondary fibers are generated from the differentiation of epithelial cells in the equatorial region of the lens.[4,5] Prior to differentiation, epithelial cells at the equatorial region exit the cell cycle to form the secondary fibers. As the secondary fiber cells elongate and differentiate, they polarize and bend toward the equatorial epithelium, with their apical and basal tips forming adhesions with epithelial cell apical tips and the posterior capsule, respectively. Following this, the fiber cells progressively attain a concave shape while migrating toward the suture lines along the epithelium at the anterior pole and capsule at the posterior pole. During these migratory changes, the fiber cells start losing all organelles, progressively gain hexagonal symmetry, and organize into radial columns characterized by tight cell–cell adhesive interactions.[3,5] The terminally differentiated fibers not only engage in close cell–cell adhesive interactions exhibiting little to no extracellular space but also develop elaborate lateral membrane ball-and-socket interdigitations and protrusions.[3] Moreover, because there is no cell turnover in the lens, all cells generated during growth and development of this organ are retained and enclosed within a thick collagenous elastic lens capsule. Additionally, as the lens grows throughout life along with a continuous generation of secondary fibers, newly formed fibers sequentially overlay previously formed fibers, like the layers of an onion.[3] Although an unparalleled degree of symmetry in the cytoarchitecture of the lens fibers including radial alignment and hexagonal shape is believed to be critical for the optical properties of lens, the biomechanical and contractile properties of fiber cells are also critical for lens shape changes associated with visual accommodation, indicating the importance of both cell adhesive interactions and cytoskeletal organization for maintenance of lens architecture and function.[6,7]

Both lens epithelium and fibers develop extensive cadherin-based cell–cell adhesive interactions referred to as adherens junctions (AJs). Although the lens epithelium develops both E-

cadherin– and N-cadherin–based AJs, fiber cells express only N-cadherin and form N-cadherin–associated AJs.[8,9] Membrane cadherins interact with cytoplasmic catenins, which in turn bind to cytoskeletal proteins.[2] The extracellular domains of cadherins engage in a calcium dependent homophilic interaction with identical cadherins from an adjacent cell, whereas their cytoplasmic tails bind to Armadillo catenins (including p120 and β- and γ-catenins).[1,2] β-Catenin interacts with α-catenin, which contains an actin-binding domain and links AJ complexes to the actin cytoskeleton.[10,11] Although maturation of N-cadherin–based AJs is reported to be required for lens fiber cell differentiation and shape change,[8,12,13] gene targeting studies have demonstrated a requirement for E-cadherin, N-cadherin, and β-catenin for lens morphogenesis, fiber cell differentiation, and architecture.[14–16] Although α-catenin has been shown to interact with AJs in lens fibers, information on expression and distribution profiles of α-catenin subtypes and their role in lens morphogenesis and architecture is lacking.[8,17,18] Unlike the Armadillo catenins (e.g., p120 catenin, β-catenin, and γ-catenin), α-catenins lack an Armadillo domain, belong to the vinculin superfamily of proteins, and regulate the stability and dynamics of AJs by linking the actin cytoskeleton directly or indirectly to β-catenin.[10,19] Three different types of α-catenins exhibiting tissue preferred expression patterns have been identified including αE-catenin (epithelial), αN-catenin (neural), and αT-catenin (testis).[10] These proteins are encoded by the *CTNNA1*, *CTNNA2,* and *CTNNA3* genes, respectively. In addition to their role in linking the actin cytoskeleton to AJs, the α-catenins also play a crucial role in mechanotransduction and cell signaling by serving as force transducers.[2,11,20–22] In rodents, αN-catenin exists as two isoforms exhibiting molecular masses of 102 (isoform I) and 113 kDa (isoform II). In adulthood, however, isoform I is found to be predominant, whereas isoform II appears to be down-regulated during development in mice.[23] In humans, an additional isoform with a molecular mass of 65 kDa is observed in addition to the 102- and 113-kDa isoforms of αN-catenin.[24]

Although α-catenin has been shown to be expressed in and to associate with AJs in the lens, it is not clear whether lens fibers express αE-catenin or αN-catenin or both types of the protein.[8,17] Toward this, in our ongoing work on characterization of lens fiber cell membrane cytoskeletal scaffolding proteins, we identified αN-catenin in immunoprecipitates of periaxin and Ankyrin-B[25] and in lipid rafts isolated from lens tissue. Moreover, we also found a relatively moderate level of *CTNNA2* gene expression in both neonatal and adult mouse lenses based on cDNA microarray analysis. Because αN-catenin is expressed primarily in neuronal cells,[23,26] and our studies indicate that the protein is not only expressed but also coimmunoprecipitates with periaxin and Ankyrin-B in the lens, we characterized the distribution pattern of αN-catenin in developing and mature lenses and evaluated its interaction with AJs proteins and the stability of AJs in the absence of periaxin, to address the role of the former in lens architecture and function.

Materials and Methods

Mice

Studies were performed in compliance with the ARVO Statement for the Use of Animals in Ophthalmic and Vision Research and with approval of the Duke University Medical Center Institutional Animal Care and Use Committee (IACUC). Mice (C57/BL6 strain) were maintained in a pathogen-free vivarium under a 12-hour dark and light cycle with ad libitum food and water. At required gestational ages, fetuses were removed by hysterectomy after the dams had been anesthetized with Euthasol (Cat. No. NDC-051311-050-01; Virbac AH, Inc., Fort Worth, TX, USA). Periaxin-null mice (C57/BL6 genetic background) were used as described previously by us.[25]

Human Donor Lenses

The use of human lenses in this study was in accordance with the tenets of the Declaration of Helsinki and adhered to the requirements of the HIPPA guidelines.

RT-PCR

To determine the expression of αN-catenin in lens tissue, total RNA was extracted from neonatal (P2) and P21 mouse lenses using an RNeasy Micro kit (Cat. No. 74004; Qiagen, Inc., Valencia, CA, USA) and reverse transcribed using the Advantage RT for PCR Kit (Cat. No. 639506; Clontech Laboratories, Inc., Mountain View, CA, USA), as we described previously.[27] Reverse-transcribed single-stranded cDNA and gene-specific forward and reverse oligonucleotide PCR primers (Supplementary Table S1) were used to amplify the different splice variants (encoding isoforms I and II) of αN-catenin. The amplified DNA products were separated on an agarose gel and visualized with GelRed Nucleic Acid Stain (Cat. No. 41002; Biotium, Hayward, CA, USA) using a Fotodyne Trans-illuminator (Fotodyne, Inc., Hartland, WI, USA). Amplified DNA products were sequenced to confirm identity.

Immunoprecipitation and Mass Spectrometry

To identify αN-catenin and N-cadherin–interacting proteins in lens, we performed immunoprecipitation analyses using anti-rat αN-catenin monoclonal antibody and anti-mouse N-cadherin monoclonal antibody (see Supplementary Table S2 for details), along with their respective IgG controls and adult mouse lens homogenates as we previously described.[25] Immunoprecipitates were separated on gradient SDS-PAGE and stained with gel code blue, and protein bands were in-gel digested with trypsin.[25] Trypsin digested protein samples were analyzed by liquid chromatography–tandem mass spectrometry (LC-MS/MS) using a nanoAcquity ultra performance liquid chromatography system coupled to a Synapt G2 HDMS mass spectrometer (Waters Corp., Milford, MA, USA) as we described previously.[25] Immunoprecipitates were also subjected to immunoblot analyses to confirm the presence of selected proteins identified by mass spectrometry.

Immunoblot Analysis

To determine the levels of αN-catenin and αE-catenin proteins in lens epithelium and fibers, adult mouse lenses were microdissected to isolate the capsule and attached epithelium and the fiber mass using a fine forceps and a tissue-dissecting microscope. Additionally, to determine the distribution of αN-catenin in lens-soluble and membrane-enriched fractions, lenses (from P21, P120, and 5-month-old periaxin-null and wild-type mice) were homogenized using a Dounce glass homogenizer and cold (4°C) hypotonic buffer containing 10 mM Tris buffer, pH 7.4, 0.2 mM $MgCl_2$, 5 mM N-ethylmaleimide, 2.0 mM sodium orthovanadate, 10 mM sodium fluoride, 60 μM phenylmethylsulfonyl fluoride, 0.4 mM iodoacetamide, protease inhibitor cocktail (complete, Mini, EDTA free), and PhosSTOP phosphatase inhibitor cocktail (one each/10 mL buffer; obtained from Roche, Manheim, Germany). The lens capsule was also homogenized as described above. Homogenates were processed for extraction of the 800*g* fraction or separation of soluble (100,000*g* supernatant) and

Investigative Ophthalmology & Visual Science

membrane-enriched fractions (100,000*g* pellet) as described previously.[28] Protein concentrations were estimated using protein assay reagent (Bio-Rad, Hercules, CA, USA), and samples were separated by SDS-PAGE (8% and 10% acrylamide gels), followed by electrophoretic transfer to nitrocellulose membrane, which were blocked and incubated with primary antibodies including αN-catenin, N-cadherin, αE-catenin, β-catenin, ankyrin-B, ARVCF, β2-Spectrin, and glyceraldehyde 3-phosphate dehydrogenase (GAPDH; see Supplementary Table S2 for details), in conjunction with horseradish peroxidase–conjugated secondary antibodies.[28] Detection of immunoreactivity was based on enhanced chemiluminescence. Densitometric analysis of immunoblots was performed using ImageJ software (http://imagej.nih.gov/ij/; provided in the public domain by the National Institutes of Health, Bethesda, MD, USA). Data were normalized to the specified loading controls. To normalize for membrane protein loading (L control), equal amounts of membrane-enriched samples from different samples were resolved by SDS-PAGE and stained with Coomassie Brilliant Blue R-250, and protein bands detected at 36 and 20 kDa were used for normalization.

A transparent human lens from a 56-year-old donor, obtained from a local eye bank (Miracles In Sight, Winston-Salem, NC, USA), was microdissected into four fractions (L1: capsule, L2: outer cortical region, L3: inner cortical region, and L4: nucleus), which were homogenized as described above. The 800*g* supernatant from each of the homogenates was immunoblotted to determine levels of αN-catenin as described above. The presence of αN-catenin was also evaluated by immunoblot analysis of 800*g* supernatants obtained from additional lenses (donors aged 19 and 31 years old).

Tissue Fixation and Sectioning

Mouse tissue specimens (embryonic heads and eyes) were fixed for cryosectioning in 4% buffered paraformaldehyde for 24 hours at 4°C, transferred into 5% and 30% sucrose in PBS on successive days, embedded in optimal cutting temperature (OCT) embedding media (Tissue-Tek, Torrance, CA, USA), and cut into 8- to 10-μm-thick sections using Microm HM550 Cryostat (GMI, Ramsey, MN, USA), as we previously described.[25] Normal human lens (from a 25-year-old donor obtained from Miracles In Sight) was fixed in 4% buffered paraformaldehyde for 2 hours at 4°C and split into two halves using a thin steel blade, followed by continued fixation in paraformaldehyde for 24 hours, transfer into 5% and 30% sucrose on successive days, embedding in OCT, and sectioning as described above.

Additionally, freshly enucleated eyes from P21 mice were fixed in 3.7% buffered formalin, embedded in paraffin, and cut into 5-μm-thick sections (equatorial plane) as we described previously.[25]

Immunofluorescence Analysis

Air-dried tissue cryosections were treated with Image-iT FX signal enhancer (Invitrogen, Eugene, OR, USA) and blocked using blocking buffer (5% globulin-free BSA and 5% filtered goat serum in 0.3% Triton X-100 containing PBS) for 30 minutes each.[27] Tissue sections were then incubated overnight at 4°C with 1:200 dilutions of primary antibodies in blocking buffer, including αN-catenin, αE-catenin, periaxin, and N-cadherin (see Supplementary Table S2 for details). Sections were then washed in 0.3% Triton X-100 containing PBS prior to incubation with appropriate Alexa Fluor (488 or 594)–conjugated secondary antibodies. For F-actin staining, preblocked sections were labeled with tetra rhodamine isothiocyanate–conjugated phalloidin (TRITC Cat. No. P1951; Sigma Aldrich Corp., St. Louis, MO, USA) for 2 hours at 1:500 time dilution, washed, and mounted as described above. All representative immunofluorescence data reported in this study are based on analysis of a minimum of three tissue sections derived from two independent specimens. Images were captured using an Eclipse 90i confocal laser scanning microscope (Nikon Instruments, Inc., Melville, NY, USA).

For paraffin sections, deparaffinization and antigen retrieval were performed as we described earlier.[25] Tissue sections were blocked for 10 minutes in a humidified chamber with medical background Sniper reducing solution (Biocare Medical, Concord, CA, USA), prior to incubation for 24 hours at 4°C with anti-rabbit polyclonal αN-catenin antibody along with one of the following mouse-monoclonal antibodies for colocalization analyses: N-cadherin, β-actin, β-catenin, ankyrin-B, β-spectrin, or Armadillo repeat protein deleted in velo-cardio-facial syndrome homolog (ARVCF; Supplementary Table S2). For periaxin colocalization with αN-catenin and N-cadherin, tissue sections were incubated with periaxin antibody and αN-catenin antibody (anti-rat) or with anti-rat monoclonal N-cadherin antibody (see Supplementary Table S2 for details). Tissue sections were washed in TBS (Tris-buffered saline) buffer and incubated with either Alexa Fluor 488– or 594–conjugated secondary antibodies (Invitrogen, Grand Island, NY, USA; at a 1: 200 dilution) in a dark humidified chamber for 2 hours at room temperature. After this, sections were washed again with TBS buffer, and slides were mounted using Vecta mount and nail polish and imaged using a Nikon Eclipse 90i confocal laser scanning microscope to obtain single optical images as previously described.[28]

For three-dimensional (3D) reconstruction, the immunostained sections were imaged at room temperature using a Zeiss 780 inverted confocal microscope (Carl Zeiss Microscopy, LLC, Oberkochen, Germany) equipped with Argon/2, 561-nm diode lasers, and a 100×, 1.40 numerical aperture Oil Plan-Apochromat DIC lens (zoom 3). Images were acquired using ZEN Black 2011 imaging software (Carl Zeiss Microscopy, LLC, Thornwood, NY, USA) as previously described.[28] For viewing fiber cells, Z-stack images were captured at a 0.2-μm step interval at a depth of 100 μm from the epithelium, and 25 to 30 optical sections were collected. The captured Z-stacks were processed using Volocity 6.3.1 software (Perkin Elmer, Waltham, MA, USA). Deconvoluted images were used for the 3D reconstruction and processed using Adobe Photoshop version CS4 (Adobe, San Jose, CA, USA).[28]

Statistical Analysis

Data from immunoblot quantification were analyzed by the Student's *t*-test, and $P < 0.05$ was considered to define statistically significant differences between two different samples. Values are presented as mean ± SD.

Results

Expression and Distribution of αN-Catenin in Mouse Lens

The requirement of cadherin/catenin-based cell adhesive interactions for lens morphogenesis, differentiation, and architecture has been well documented.[8,14,16] However, it is not clear with respect to expression and distribution of different subtypes of α-catenin and their role in lens which play a key role in recruitment of actin cytoskeleton to AJs.[11] Having repeatedly observed the presence of αN-catenin in immunoprecipitates of ankyrin-B and periaxin and in lipid rafts derived from mouse lens tissue (Pratheepa Kumari and Rao,

Investigative Ophthalmology & Visual Science

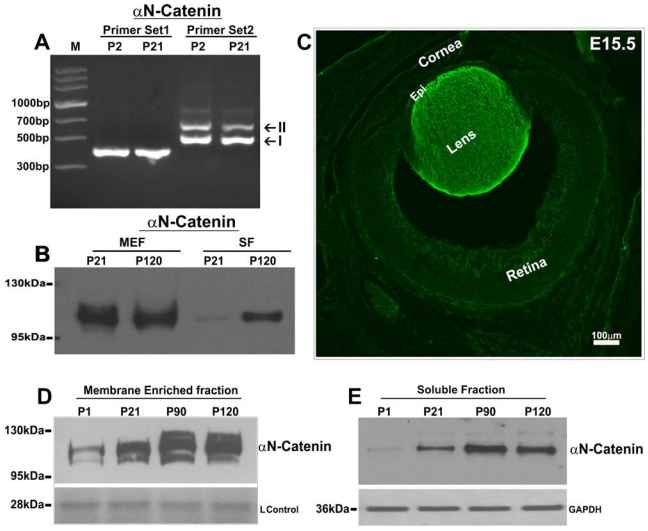

Figure 1. Expression and distribution of αN-catenin in mouse lens. (**A**) Confirmation of the expression of αN-catenin splice variants encoding isoforms I (lower band) and II (upper band) in P2 and P21 mouse lenses by RT-PCR analysis. The other weak DNA bands above the band II were found to be nonspecific based on sequence. (**B**) Distribution of αN-catenin in the membrane-enriched insoluble fraction (MEF) and soluble fraction (SF) of mouse lens from P21 and P120 based on immunoblot analysis. (**C**) Immunofluorescence-based distribution of αN-catenin in E15.5 mouse lens. *Scale bar* indicates image magnification. (**D**, **E**) Lens maturation associated changes in αN-catenin in the membrane-enriched insoluble and soluble fractions of mouse lenses derived from different age groups. "L Control" in **D** represents the loading control for the lens membrane-enriched fraction. For the soluble fractions (**E**), GAPDH was probed as a loading control.

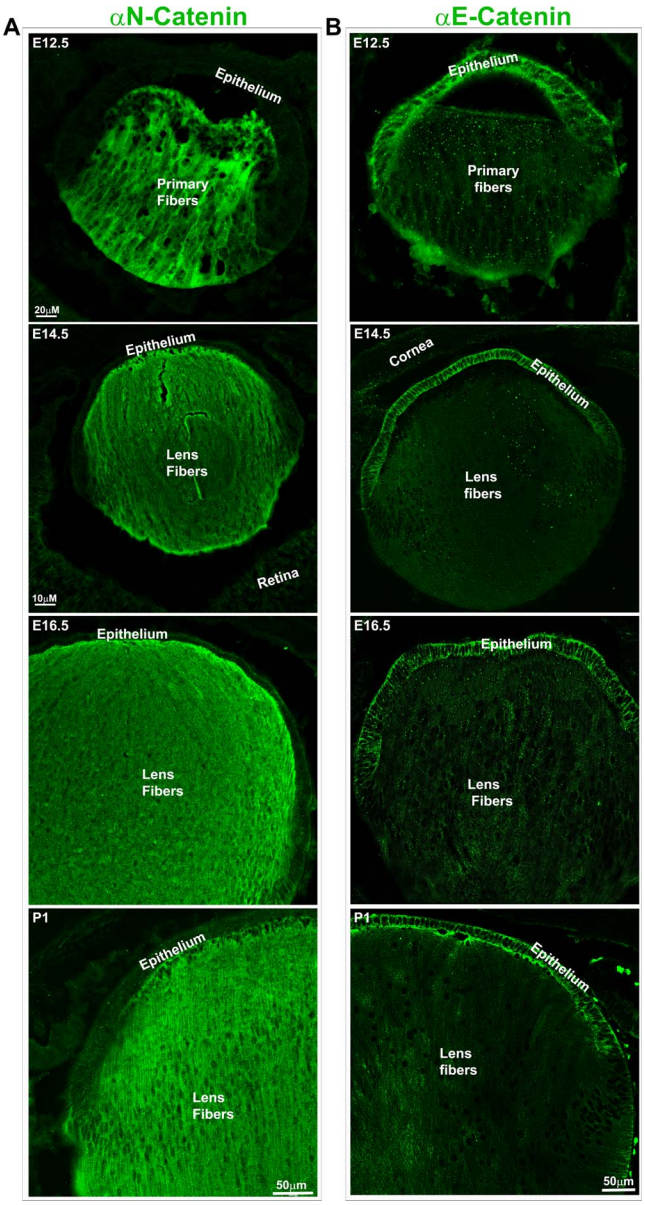

Figure 2. Discrete distribution of αN-catenin and αE-catenin in the developing mouse lens. To compare and contrast the distribution pattern of αN-catenin (**A**) with αE-catenin (**B**) in the developing mouse lens, cryosections derived from different embryonic stages and P1 mouse eyes were immunostained with αN-catenin or αE-catenin antibodies in conjunction with a secondary antibody conjugated with Alexa Fluor-488 (*green*). Representative immunofluorescence images are shown. All images are captured at a 40× magnification. *Scale bars* indicate image magnification.

unpublished data, 2017), we assessed the expression of neuronal specific αN-catenin in mouse lenses initially by analysis of cDNA microarray (mouse genome 430 2.0 array; Affymetrix, Thermo Fisher Scientific, Waltham, MA, USA) data generated previously in our laboratory (deposited in NCBI/National Institutes of Health cDNA microarray database, GEO accession #GSE99218) and by RT-PCR analysis, as not much is known about this catenin in lens. αN-catenin, which is encoded by *CTNNA2,* was found to be expressed in both neonatal (P7) and adult (2 months old) mouse lenses exhibiting relative signal intensities (RSIs) of 2305 and 6421, respectively. Of the three known subtypes of α-catenin, expression of αE-catenin (encoded by *CTNNA1*) was found to be higher than that of αN-catenin in both P7 (RSI: 10203) and adult mouse (RSI: 11182) lens by approximately 4- and 2-fold, respectively. αT-catenin (encoded by *CTNNA3*), in contrast, exhibited a minimal level of expression (RSI; <80) compared with both αE- and αN-catenins. We also performed RT-PCR analysis to confirm the expression of *CTNNA2* splice variants (encoding isoforms I and II) in P2 and P21 mouse lenses using two different sets of gene-specific oligonucleotide PCR primers. Unlike set 1 primers, which were chosen to amplify the splice variant encoding isoform I of αN-catenin, set 2 primers are known to amplify two different splice variants encoding both isoforms (I and II) of αN-catenin.[23] αN-catenin II (113 kDa) has been shown to have a 48-amino-acid insertion in its C-terminal region relative to αN-catenin I (molecular mass of 102 kDa).[23] Figure 1A shows expression of αN-catenins splice variants in P2 and P21 mouse lenses with relatively higher expression of splice variants I (encoding isoform I) than splice variant 2 (encoding isoform II).

Having confirmed the expression of the *CTNNA2* gene in mouse lens, we then evaluated for the presence of αN-catenin in the mouse lens epithelium, fiber mass, and soluble and insoluble membrane-enriched fractions by immunoblot analyses using anti-rat monoclonal αN-catenin antibody. Both the lens membrane-enriched fractions and soluble fractions (20 μg protein; P21 and P120 mice) exhibited a specific immunopositive protein band at around 102 kDa with a relatively higher concentration in the membrane-enriched fraction compared with the soluble fraction (Fig. 1B). Additionally, within the lens, αN-catenin is distributed primarily to the fibers, with little to none detected in the epithelium based on both immunofluorescence using E15.5 mouse specimen (Fig. 1C) and immunoblot analyses in P21 mouse lens (Figs. 2A, 3A).

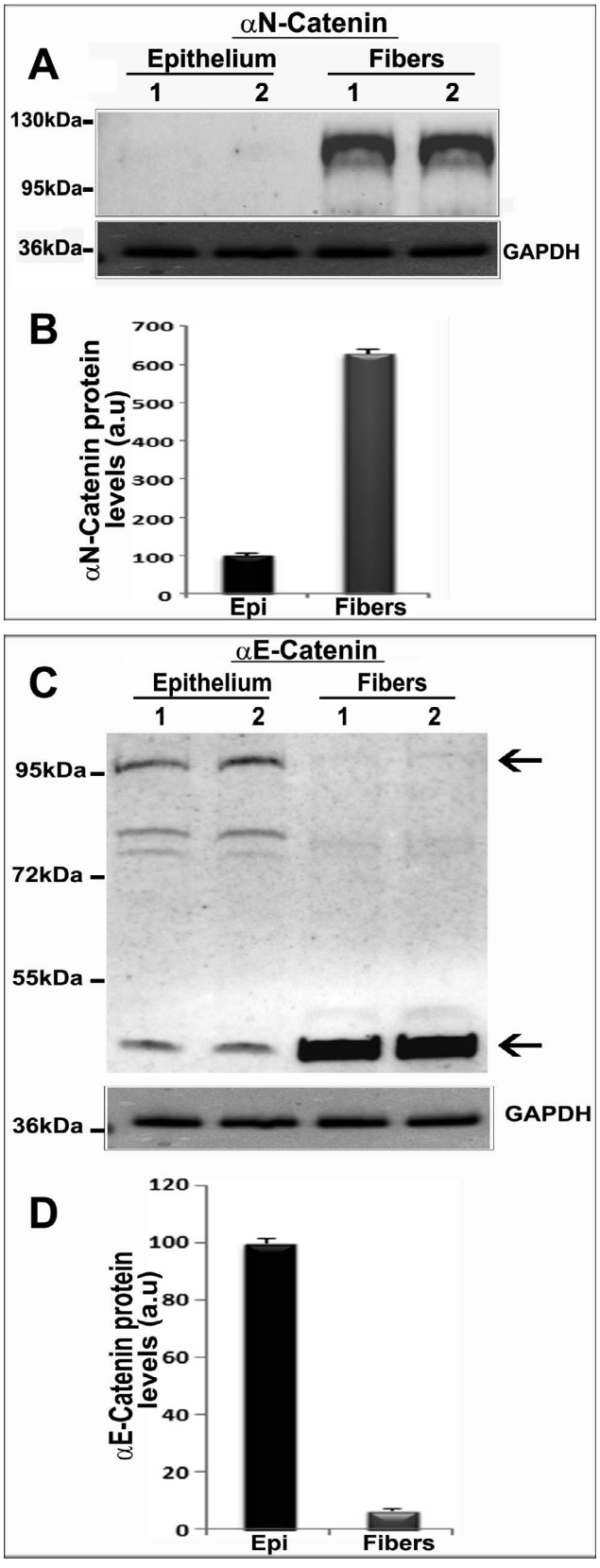

Figure 3. Distribution of αN-catenin and αE-catenin in the epithelial and fiber mass fractions of mouse lens. (**A**) Distribution of αN-catenin in the epithelial and fiber mass fractions (800*g* supernatant) of two independent (lanes 1 and 2) P21 mouse lens samples. (**B**) Quantitative changes in αN-catenin protein levels between epithelial and fiber mass fractions of mouse lens. (**C**) Distribution of αE-catenin in the lens epithelium and fiber mass by immunoblot analysis using the respective tissue homogenates derived from P21 mouse lens described in **A**. The *upper arrow* points to the expected native form of αE-catenin. The *lower arrow* indicates the nonspecific immunoreactivity to the αE-catenin antibody used. Lanes 1 and 2 represents two independent samples. (**D**) Quantitative differences in the levels of αE-catenin between the lens epithelium and fiber mass based on densitometric analysis of immunoblots shown in **C**. GAPDH was probed as a loading control. Values are mean ± SD based on two pooled samples. a.u., arbitrary units.

Data shown in Figure 3A are based on two independent pooled P21 samples (for epithelium and fiber mass, four and two lenses were pooled per sample, respectively; 10 μg protein was analyzed), and values are mean ± SD and normalized to the values of GAPDH (Fig. 3B).

Lens maturation-dependent changes in αN-catenin were also examined by immunoblotting analysis using lens specimens derived from P1, P21, P90, and P120 mice. The levels of αN-catenin gradually increased from P1 to P90 and plateaued by P120 (20 μg protein; Figs. 1D, 1E), in both membrane-enriched insoluble and soluble fractions. Proteins from membrane fraction samples were normalized to one of the Coomassie blue–stained membrane protein bands separated by SDS-PAGE. Protein data from the soluble fractions were normalized to GAPDH. It is noteworthy that membrane-enriched fractions exhibited multiple, but closely migrating, immunopositive bands corresponding to αN-catenin, with molecular masses between 100 and 120 kDa, suggesting maturation-dependent posttranslational processing of membrane-associated αN-catenin may occur in lens fibers (Fig. 1D).

Differential Distribution of αN- and αE-Catenins in the Epithelium Versus Fiber Cell Mass of Developing Mouse Lens

To determine the expression and distribution pattern of αN-catenin in the developing mouse lens, cryosections derived from E12.5, E14.5, E6.5, and P1 mouse eye specimens were immunostained using a rabbit polyclonal anti–αN-catenin antibody. As can be seen in Figures 1C and 2A, there is an abundant and diffuse distribution of αN-catenin–specific immunofluorescence (green) primarily in the lens fibers (both primary and secondary), which appears to undergo a robust up-regulation during the elongation and differentiation of lens fiber cells. During development of the eye (starting from E12.5 to E16.5), the lens tissue exhibits intense staining for αN-catenin expression relative to all other ocular tissues (Figs. 1C, 2A).

In contrast to αN-catenin, αE-catenin, an E-cadherin binding protein in developing (E12.5, E14.5, and E16.5), and P1 mouse lenses showed a discrete and intense distribution to the epithelium based on immunofluorescence analysis of cryosections using rabbit polyclonal antibody (Fig. 2B). Within the lens epithelium, αE-catenin is localized primarily to the cell–cell junctions. Consistent with the immunofluorescence data (Fig. 2B), immunoblot analysis of 800*g* supernatants from P21 mouse lens using αE-catenin antibody revealed that this protein distributes primarily to epithelial fractions with very little present in the lens fiber cell mass (10 μg protein; Figs. 3C, 3D). In Figure 3C, the upper arrow points to the expected molecular mass of αE-catenin. In addition to a prominent band at 95 kDa, there are additional bands at ~80 kDa and below 55 kDa in the lens epithelium. As per the product datasheet provided by the reagent manufacturer, the αE-catenin antibody used in this study has been shown to recognize a 50-kDa protein of unknown origin. The values in Figure 3D represent a

Investigative Ophthalmology & Visual Science

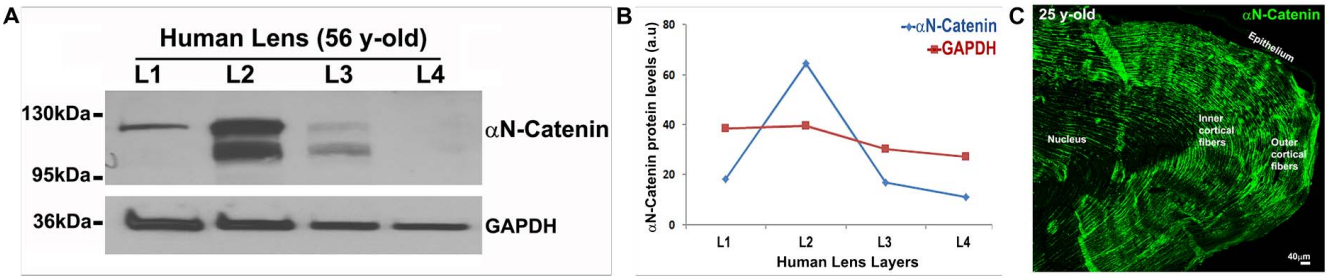

FIGURE 4. Lens maturation dependent changes in distribution and stability of αN-catenin in human donor specimens. (**A**) To examine the distribution and stability of αN-catenin within different regions of the lens, human donor lenses were microdissected into four layers representing epithelium (L1), outer cortex (L2), inner cortex (L3), and nucleus (L4), and the respective homogenates (800*g* supernatants) were immunoblotted for αN-catenin. GAPDH was also immunblotted for a housekeeping protein. (**B**) Densitometry-based quantitative changes in αN-catenin in the L1 to L4 layers of human lens described in **A**. a.u., arbitrary units. (**C**) Cryosections of human lens from a 25-year-old donor were immunostained for αN-catenin (*green*) distribution. *Scale bar* denotes 40 μm.

mean of two independent pooled specimens as described in Figures 3A and 3B.

Maturation-Dependent Changes in Patterns of αN-Catenin Expression in Human Lenses

Maturation-dependent changes in αN-catenin distribution within the lens were also evaluated in human specimens (Fig. 4A). Transparent human lenses derived from a 56-year-old donor were microdissected into four fractions (layers 1 to 4; representing epithelium, outer cortex, inner cortex, and nucleus, respectively), and the 800*g* supernatants of tissue homogenates (20 μg protein) were used to determine the levels of αN-catenin by immunoblot analysis. The same samples were also immunoblotted for GAPDH. Compared to the L1 (epithelium) fraction, the L2 (outer cortex) fraction exhibited high levels of αN-catenin, with levels decreasing progressively and dramatically in layers L3 and L4 relative to those in L2 (Fig. 4A). Interestingly, although fraction L1 contains a single immunopositive αN-catenin protein band, fractions L2 and L3 reveal two distinct closely migrating bands of αN-catenin. Whether the second protein band is the result of posttranslational modification, proteolytic cleavage of αN-catenin, or if the bands represent isoforms of αN-catenin is not clear. Figure 4B summarizes changes in protein levels of αN-catenin protein (results of densitometric analysis) relative to GAPDH protein levels across different layers of the human lens. The presence of αN-catenin in human lenses was also confirmed by immunoblot analysis of 800*g* supernatants derived from additional donor lenses (donors aged 19 and 31 years old; data not shown). Figure 4C shows the distribution pattern of αN-catenin in a 25-year-old human lens by immunofluorescence analysis using sagittal plane cryosections (image captured with 10× magnification). Consistent with the immunoblot data, intense staining for αN-catenin is evident throughout the outer cortical fibers, with a gradual reduction observed in the inner cortical region and nuclear regions. Similar to data obtained from the mouse lens, human lens epithelium exhibits almost no immunostaining for αN-catenin. Therefore, in Figure 4A, the anti–αN-catenin immunoreactive band in the L1 layer could be the result of fiber cell contamination of the epithelial fraction.

Identification and Colocalization Analysis of αN-Catenin and N-Cadherin Interacting Proteins in the Mouse Lens

To identify and characterize proteins that interact with αN-catenin, we performed immunoprecipitation analyses using mouse lens homogenates and an αN-catenin rat monoclonal antibody as described in the methods section. Immunoprecipitates were separated by gradient SDS-PAGE, followed by in-gel trypsin digestion of separated protein bands and mass spectrometric identification of individual peptides. Additionally, the profile of proteins pulled-down by the αN-catenin antibody was compared to that coimmunoprecipitated from lens homogenates by the N-cadherin antibody (Table). Based on peptide profiles generated via mass spectrometry analysis, it is evident that αN-catenin and N-cadherin reciprocally coimmunoprecipitate from lens homogenates. Several additional proteins were found to be common across coimmunoprecipitates obtained using αN-catenin and N-cadherin antibodies including β-catenin, plectin, spectrin (both α and β), dynein 1 heavy chain 1, Rho guanine nucleotide exchange factor 38, bifunctional uridine diphosphate (UDP)-*N*-acetylglucosamine transferase and deubiquitinase (ALG13), small heat shock protein-1, Golgi-associated PSD-95, discs-large, ZO-1 (PDZ) and coiled-coil motif–containing protein (GOPC). In addition to these common proteins, αN-catenin antibody also pulled down A-kinase anchor protein 9 (AKAP9), NrCAM, ATP-binding cassette subfamily A member 9 (ABCA9), Armadillo repeat protein deleted in velo-cardio-facial syndrome homolog (ARVCF), vinculin, lengsin, Ankyrin-2, and lens fiber membrane intrinsic protein (LMIP). Likewise, N-cadherin antibody also pulled-down certain unique proteins including E3 ubiquitin-protein ligase UBR4, aquaporin-0, and α-enolase. In addition to mass spectrometry–based identification, we also confirmed the presence of αN-catenin, N-cadherin, β-spectrin, β-catenin, ankyrin-B, and ARVCF in αN-catenin immunoprecipitates by immunoblot analyses (Supplementary Fig. S1). Similarly, the presence of αN-catenin, N-cadherin, β-spectrin, and β-catenin in N-cadherin immunoprecipitates was confirmed by immunoblotting analyses (Supplementary Fig. S1).

Following identification of proteins that coimmunoprecipitated with αN-catenin, we examined the colocalization of selected proteins with αN-catenin by immunofluorescence and confocal imaging (Fig. 5). In P21 mouse lens cryosections (sagittal plane; images with 10× magnification), αN-catenin colocalized with N-cadherin and actin (stained with rhodamine-phalloidin) in lens fibers, as evidenced by the merged images in Figures 5A and 5B. Additionally, in equatorial plane sections from P21 mouse lenses (paraffin-embedded), αN-catenin staining was noted to be distributed throughout the hexagonal fibers cells including both the short and long arms of fibers cells. Further, similar to the colocalization pattern noted in sagittal sections, equatorial plane sections exhibit obvious colocalization of αN-catenin and N-cadherin (images captured with 100× magnification), based on the merged

Investigative Ophthalmology & Visual Science

Table. Mass Spectrometry–Based Identification of αN-Catenin and N-Cadherin Coimmunoprecipitated Proteins From the Mouse Lens Homogenates

Identified Proteins	Accession Number	Molecular Weight, kDa	Mouse IgG	N-Cadh IP, Peptides, *n*	Rat IgG	αN-Catenin IP, Peptides, *n*
Cluster of Catenin α-2	CTNNA2	105	0	66	0	58
Catenin β-1	CTNNB1	85	0	31	0	31
Plectin	PLEC	534	0	5	1	31
Putative bifunctional UDP-*N*-acetylglucosamine transferase and deubiquitinase ALG13	ALG13	129	0	22	0	13
Spectrin α chain, nonerythrocytic 1	SPTN1	285	0	16	0	8
Cadherin-2	CADH2	100	0	9	0	13
E3 ubiquitin-protein ligase UBR4	UBR4	572	0	4	0	–
A-kinase anchor protein 9	AKAP9	436	0	–	0	8
Rho guanine nucleotide exchange factor 38	ARH38	88	0	5	0	1
Protein SYS1 homolog	SYS1	18	0	4	0	–
Lens fiber major intrinsic protein	MIP	28	0	5	0	–
Collagen α-1(IV) chain	CO4A1	161	0	4	0	–
Cytoplasmic dynein 1 heavy chain 1	DYHC1	532	0	3	0	3
Neuronal cell adhesion molecule	NRCAM	139	0	–	0	3
ATP-binding cassette subfamily A member 9	ABCA9	183	0	–	0	2
Heat shock protein β-1	HSPB1	23	0	2	0	1
Golgi-associated PDZ and coiled-coil motif-containing protein	GOPC	51	0	2	0	1
Spectrin β chain, nonerythrocytic 1	SPTB2	274	0	2	0	3
Armadillo repeat protein deleted in velo-cardio-facial syndrome homolog	ARVCF	105	0	–	0	3
α-Enolase	ENOA	47	0	2	0	–
Lengsin	LGSN	62	0	–	0	2
Vinculin	VINC	117	0	–	0	2
Ankyrin-2	ANK2	426	0	0	0	2
Lens fiber membrane intrinsic protein	LMIP	20	0	1	0	2

n = number of peptides.

images shown in Figures 5A and 5B. Likewise, although αN-catenin and β-actin also colocalize, the degree of colocalization is not as intense as that observed for αN-catenin and N-cadherin. Additionally, we also examined for colocalization of αN-catenin with N-cadherin, β-spectrin, ankyrin-B, β-catenin, ARVCF, and β-actin at high resolution (100× magnification with zoom 3 using Zen Black 2011 imaging software) with 3D reconstruction (using Volocity 6.3.1 software and image deconvolution) using paraffin-embedded equatorial plane sections of P21 mouse lenses. As can be seen from Figure 5C, although the degree of colocalization of ankyrin-B, β-catenin, and ARVCF with αN-catenin is similar at both the short and long arms of the hexagonal fiber cells from the lens cortical region, the degree of colocalization of β-spectrin, β-actin, and N-cadherin with αN-catenin is greater at the short arms of the fiber cells. Collectively, these colocalization analyses reveal that αN-catenin codistributes with N-cadherin, β-catenin, ARVCF, ankyrin-B, spectrin, and actin in the lens fibers.

Periaxin Interaction With N-Cadherin and αN-Catenin in Mouse Lens

Periaxin, a PDZ domain protein, is expressed in lens fiber-specific manner and has been shown to participate in maintaining fiber cell shape and membrane organization in coordination with ankyrin-B, spectrin, neuronal cell adhesion molecule (NrCAM), and the actin cytoskeleton.[25,28] Previously, we have reported that mass spectrometry analysis of periaxin antibody immunoprecipitates obtained from lens homogenates confirm presence of αN-catenin.[25] This observation was further confirmed in the current study (data not shown). Intriguingly, although we found that αN-catenin consistently coimmunoprecipitates with periaxin antibody, periaxin was not reciprocally coimmunoprecipitated from lens homogenates either with αN-catenin or N-cadherin antibodies. This discrepancy could be potentially related to antibody epitope masking or protein crowding. However, we previously reported the presence of ankyrin-B in immunoprecipitates of periaxin[25] and showed that ankyrin-B and αN-catenin reciprocally coimmunoprecipitate from lens homogenates (Table) (Maddala and Rao, unpublished data, 2017). Based on these multiple observations, we proceeded to analyze colocalization of periaxin with αN-catenin and N-cadherin in the mouse lens by immunofluorescence analysis. Figure 6 shows colocalization of periaxin with αN-catenin and N-cadherin in sagittal (cryosections, images with 10× magnification; Figs. 6A, 6B) and equatorial sections (paraffin sections, images with 100× magnification; Figs. 6A, 6B) of P21 mouse lenses. Moreover, in high-resolution 3D reconstruction images, the colocalization between periaxin and αN-catenin, especially at vertices, is obvious and intense (see arrows in Fig. 6C). Similarly, periaxin exhibits colocalization with N-cadherin at both the short and long arms of the hexagonal fiber cells (Fig. 6D). Collectively, these observations reveal that periaxin colocalizes to the N-cadherin/αN-catenin×based AJs in lens fibers.

Disruption of AJs in Periaxin-Deficient Mouse Lenses

The results obtained in our studies indicate that interactions among αN-catenin, N-cadherin, ankyrin-B, periaxin, and spectrin-actin cytoskeleton in lens fibers very likely influence fiber cell cytoarchitecture and adhesion.[25,28] Based on these observations, we speculated that periaxin deficiency might affect the stability of AJs in lens fibers. To explore this possibility, we compared the levels of αN-catenin, N-cadherin,

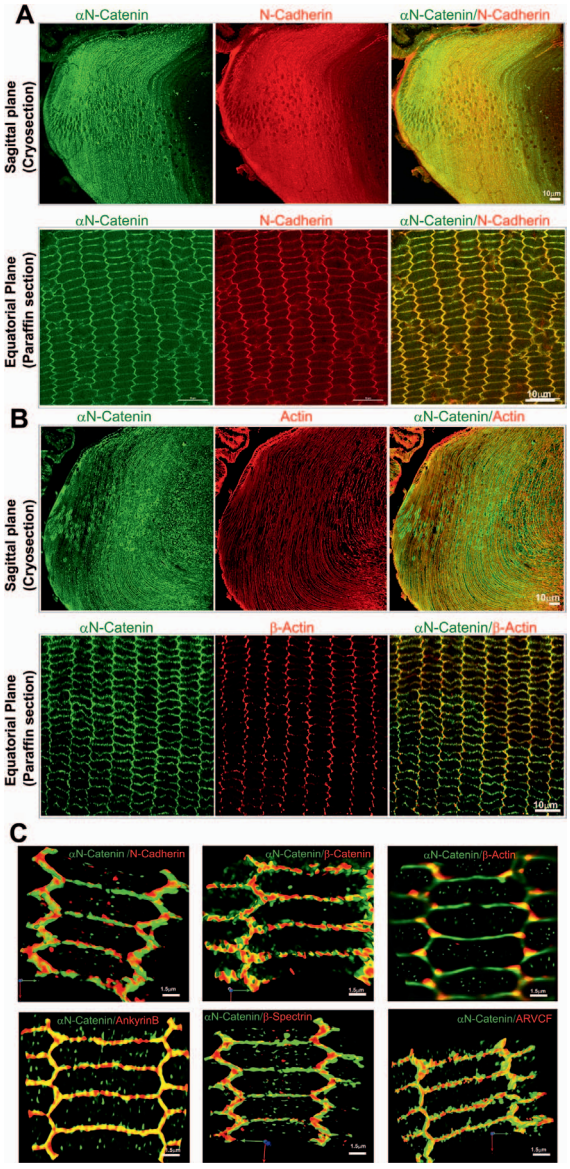

Figure 5. Colocalization of αN-catenin with AJs and other proteins in mouse lens fibers. Mouse lens (derived from P21) sagittal (cryo) and equatorial (paraffin) sections were coimmunostained for αN-catenin and N-cadherin (**A**) or αN-catenin and actin (**B**) to examine colocalization using appropriate primary and Alexa Fluor–conjugated secondary antibodies. (**C**) 3D reconstruction of deconvoluted images of lens equatorial sections (derived from P21 mouse) that were coimmunostained for αN-catenin and N-cadherin, β-catenin, β-actin, Ankyrin-B, β-spectrin, or ARVCF. *Scale Bars* show respective magnification scale.

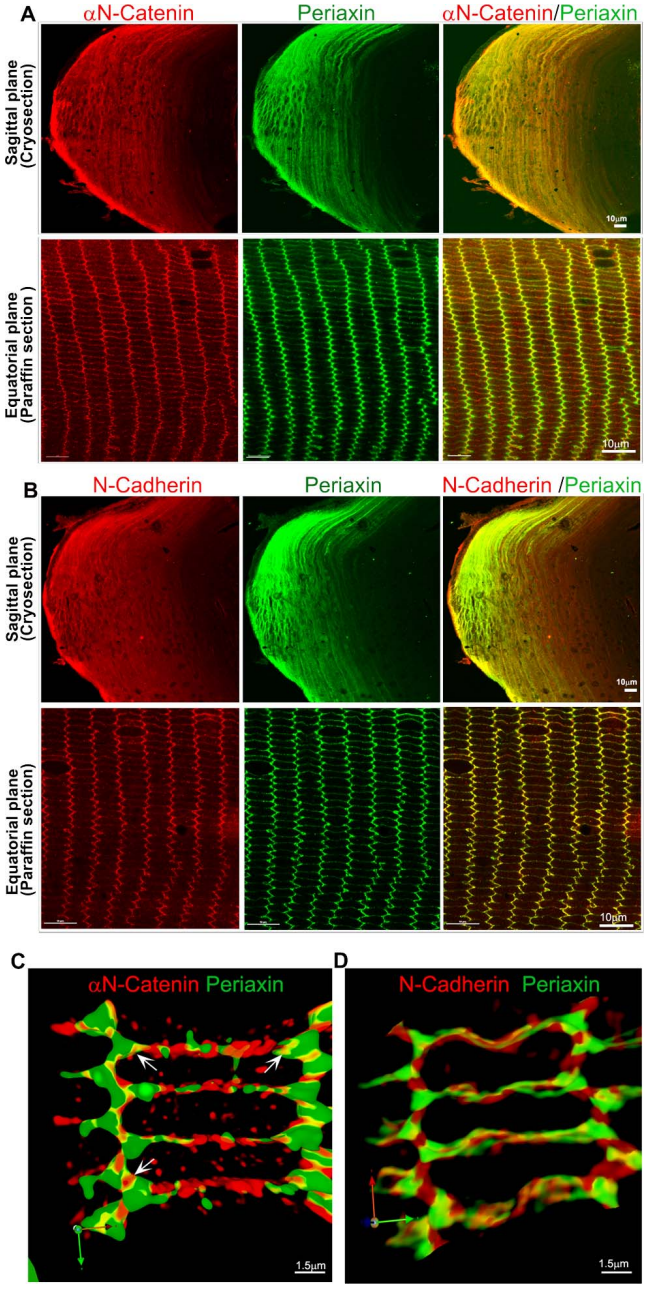

Figure 6. Colocalization of periaxin with N-cadherin and αN-catenin in mouse lens fibers. Lens sagittal (cryo) and equatorial (paraffin) sections derived from P21 mice were coimmunostained for periaxin and αN-catenin (**A**) or periaxin and N-cadherin (**B**) using appropriate primary and Alexa Fluor–conjugated secondary antibodies. (**C**, **D**) 3D reconstruction of deconvoluted images of equatorial lens sections (derived from P21 mouse) that were coimmunostained for periaxin, αN-catenin, and N-cadherin. *Scale Bars* show respective magnification scale.

β-catenin, and ARVCF (20 μg protein) in the membrane-enriched insoluble fraction of periaxin-null mouse lenses and age-matched wild-type lenses using quantitative immunoblot analysis. Previously, we demonstrated impairment of hexagonal geometry and radial arrangement of lens fiber cells in mice lacking periaxin.[25,28] Lenses derived from 5-month-old periaxin-null mice showed a significant decrease in the levels of αN-catenin (Figs. 7A, 7B; $n = 8$), N-cadherin (Figs. 7E, 7F; $n = 8$), β-catenin (Figs. 7E, 7F; $n = 8$), and ARVCF (Figs. 7E, 7F; $n = 5$) in the membrane-enriched insoluble fraction in comparison with wild-type specimens (Fig. 7). In addition to the above described changes noted in the membrane-enriched fraction of periaxin-null mouse lenses, αN-catenin levels were also evaluated in the soluble fraction of periaxin-null lenses because this protein can be detected in the soluble fraction as well (Fig. 1B). The levels of αN-catenin were found to be increased slightly (~by 30%) but significantly in the soluble fraction of periaxin-deficient mouse lenses in comparison with wild-type specimens (20 μg protein; Figs. 7C, 7D). Moreover, membrane localization of αN-catenin was found to be disrupted in periaxin-null mouse lens fibers compared with wild-type controls based on immunofluorescence analysis (Supplementary Fig. S2). Compared with αN-catenin, N-cadherin, β-

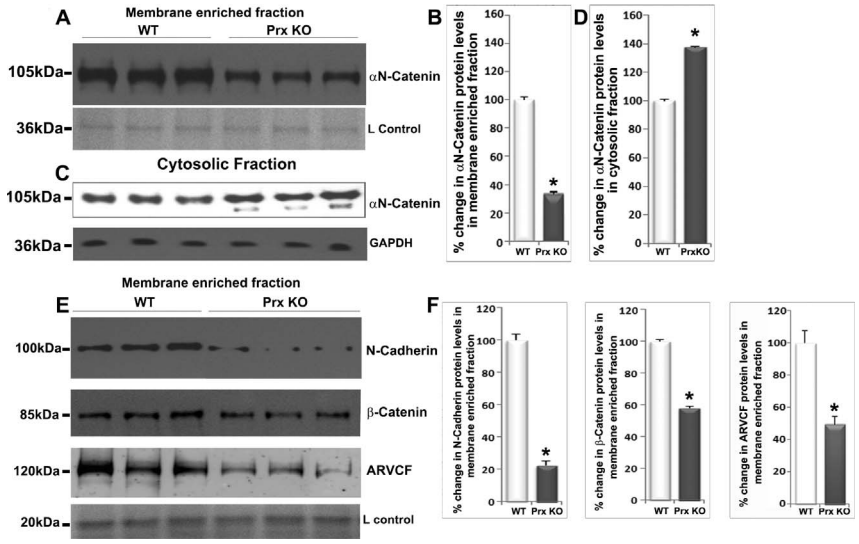

Figure 7. Periaxin deficiency affects lens fiber cell AJs. To determine the effects of periaxin deficiency on stability of AJs in lens fibers, periaxin-null and age-matched wild-type mice (5 months old) lenses were evaluated for quantitative changes in the levels of αN-catenin (**A**, **B**; $n = 8$), N-cadherin (**E**, **F**; $n = 8$), β-catenin (**E**, **F**; $n = 8$), and ARVCF (**E**, **F**; $n = 5$) proteins in membrane-enriched fractions by immunoblot with densitometric analyses. Quantitative changes in αN-catenin protein levels were also evaluated in lens soluble fractions of periaxin-null and wild-type mice (**C**, **D**). GAPDH was blotted as a loading control. L Control stands for loading control. Values were mean ± SEM of five to eight independent samples. In immunoblots, three representative samples from both wild-type and periaxin-null mouse samples are shown. $^*P < 0.05$.

catenin, and ARVCF were undetectable in the soluble fraction of both the wild-type and periaxin-null mouse lenses (data not shown). Collectively, these results reveal the importance of periaxin in stabilizing N-cadherin/ αN-catenin–based AJs in lens fibers.

Discussion

Lens fiber cell elongation and differentiation have been shown to be critically dependent on the maturation and reorganization of the AJs and the interactions of these specialized structures with the cytoskeletal network.[8,12–14] Importantly, lens fibers preferentially express N-cadherin and develop N-cadherin–based AJs, with the latter being demonstrated to play a vital role in fiber cell differentiation and cytoarchitecture.[8,9,14] A number of years ago, the Maisel laboratory reported that lens epithelial cell differentiation is associated with a precipitous loss of α-catenin, a key component of AJs, along with increased Triton insolubility of N-cadherin, and speculated that lens fibers might express a novel subtype of α-catenin in place of a down-regulated α-catenin.[29] Little effort, however, has gone into identifying and characterizing a lens fiber-specific α-catenin isoform(s).[8,12,17,18] Toward this objective, we report in this study the identification of αN-catenin, a neuronal-specific α-catenin, the discrete and intense distribution of this protein to lens fibers, and the interaction of αN-catenin with N-cadherin and other AJ-associated proteins, in contrast to the restricted distribution of αE-catenin to the lens epithelium.

Having consistently observed the presence of αN-catenin in the periaxin and ankyrin-B immunoprecipitates derived from lens homogenates, and based on the presence of αN-catenin in the periaxin- and ankyrin-B–enriched lens fiber cell lipid rafts (Pratheepa Kumari and Rao, unpublished data, 2017) we embarked on characterizing αN-catenin in the lens tissue. Although it is true that not much is known about the significance of αN-catenin in the ocular lens, we did find one report in literature briefly mentioning that, although this protein is thought to be expressed specifically in the central nervous system, αN-catenin is detected in lens fibers as well.[23] The α-catenins are intracellular proteins that contain three vinculin homology domains and bind to β-catenin through their N-terminal region, whereas their C-terminal region facilitates binding to F-actin directly or indirectly.[10,11,26] In addition to binding to F-actin, α-catenins have been shown to bind to vinculin, formin-1, ZO-1, afadin, α-actinin, epithelial protein lost in neoplasm, and Rho GTPase.[2,10,19,30] The α-catenins are also known to inhibit Arp2/3-mediated actin polymerization.[31,32] The stability and dynamics of AJs is considered to be critically dependent on α-catenin–regulated linkage of AJs with the actin cytoskeletal network.[10,11,33] Consistent with an earlier report by Bagchi et al., who documented a down-regulation of α-catenin protein levels in lens fibers,[29] in this study, we report that this observation is attributable to the αE-catenin subtype, an E-cadherin binding α-catenin, which distributes predominantly to the lens epithelium and whose expression undergoes a dramatic down-regulation in fibers. On the other hand, αN-catenin exhibited discrete distribution to the lens fibers with little to none present in the epithelium in either mouse or human lenses, based on immunoblotting and immunofluorescence analyses. Significantly, αN-catenin shows a robust up-regulation during fiber cell differentiation starting from the lens vesicle, revealing an important role for this protein in fiber cell (both primary and secondary) elongation and differentiation. Moreover, the increased levels of αN-catenin observed in maturing lenses from P1 to P90 mice suggests that it is involved not only in fiber cell differentiation but also in fiber cell maturation and compaction. Although we found evidence for expression of two splice variants encoding two isoforms of αN-catenin (I and II) in the mouse lens, it is not clear whether isoform II protein levels are high enough to detect or the doublet protein bands detected in human lens represent both isoform I and II requires further investigation. The expression of αN-catenin II has been shown to be down-regulated, however, in the adult mouse brain.[23] Collectively, the dramatic shift in α-catenin subtypes, from αE-catenin to αN-catenin, during lens epithelial cell differentiation suggests a unique role for αN-catenin in the

Investigative Ophthalmology & Visual Science

morphologic changes and physiologic attributes associated with lens fiber cell differentiation.

Although it is known that both αE and αN-catenins can participate in formation of cadherin-based AJs,[26] under in vivo conditions, αN-catenin is commonly associated with N-cadherin–based AJs.[26,34] In our immunoprecipitation analyses, we found that αN-catenin and N-cadherin reciprocally coimmunoprecipitate from lens homogenates, indicating the importance of an association between N-cadherin–based AJs and αN-catenin in the lens. We also found that the αN-catenin and N-cadherin immunoprecipitates contained high levels of β-catenin but no E-cadherin. Moreover, the presence of ARVCF, vinculin, AKAP9, Rho GEF, NrCAM, and ankyrin-B in the αN-catenin immunoprecipitates indicate interaction of both AJ proteins and signaling proteins with αN-catenin in lens fibers, suggesting a role for αN-catenin not only in fiber cell adhesive interactions but also in signaling activity. Consistent with these observations, the colocalization analyses carried out using both sagittal and equatorial mouse lens sections revealed that αN-catenin codistributes with N-cadherin, β-catenin, ARVCF, actin, spectrin, and ankyrin-B. Based on these multiple observations, it is evident that lens fibers express primarily αN-catenin and that αN-catenin interacts with N-cadherin in differentiating fiber cells. Several previously published studies have, however, reported the presence of α-catenin in lens fibers.[8,17,18] It is plausible that the α-catenin antibody used in some of the previously published studies might have recognized αN-catenin present in lens fibers.

Given our results showing that αN-catenin coimmunoprecipitates and colocalizes with periaxin and ankyrin-B in lens fibers, and the finding that periaxin and ankyrin-B mutually influence fiber cell cytoarchitecture and mechanical properties,[25,28] we evaluated the stability of N-cadherin and αN-catenin and their associated proteins including β-catenin and ARVCF in periaxin-deficient mouse lenses. Periaxin deficiency appears to impair assembly and stability of AJs in lens fibers based on the significant changes observed in the levels of N-cadherin, αN-catenin, β-catenin, and ARVCF proteins in these lens fiber cells. These observations also provide important insight into the role of AJs in periaxin and ankyrin-B–mediated regulation of lens biomechanical properties.[25,28] α-Catenins are demonstrated to serve as force transducers and mechanical modulators in addition to their critical role in AJ stability.[11,20,22] Therefore, in lens fibers that contain only αN-catenin, it is conceivable that the αN-catenin most likely participates in mechanotransduction and associated signaling mechanisms including actomyosin-driven contractile activity.[35–37] In future studies, it will be important to explore whether the known force transducer activity of α-catenin is relevant for lens mechanics and shape change during accommodation. Interestingly, tropomodulin, which plays a critical role in maintaining lens architecture and mechanical properties, has also been shown to stabilize the actin cytoskeleton and to be recruited by αN-catenin to the AJ structures.[38,39]

Finally, cerebellar-deficient folia (cdf) mutant mice, which are known to have partial deletion of the *CTNNA2* gene, exhibit defects in cerebellar and hippocampal lamination.[40] There are no known reports on lens phenotype in these mice. Because the *CTNNA2*-null mice die the day after birth,[34] developing a conditional deletion is necessary to facilitate the understanding of a definitive role for αN-catenin in lens architecture and function. It is noteworthy that αN-catenin, a neuronal specific protein involved in dendritic spine morphology and synaptic activity, is abundantly expressed in lens fibers, which also develop elaborate lateral membrane interdigitations and membrane protrusions.[3,34] Additionally, several other proteins including periaxin and NrCAM, which play a vital role in Schwan cells or neurons, are also expressed in lens fiber cells.[25,41–44] Some of these proteins, together with ankyrins and membrane cytoskeletal proteins (spectrin and actin), are demonstrated to play a crucial role in membrane domain organization in neurons and other cell types.[45,46] It is worthy of mention, albeit cautiously, that our mass spectrometric analysis detected several Bassoon peptides with low confidence in immunoprecipitates of αN-catenin. Interestingly, mouse lens cDNA microarray data also revealed expression of Piccolo at a relatively higher level than Bassoon. Both Bassoon and Piccolo are two well-characterized large scaffolding proteins of the cytomatrix assembled at the active zone involved in neurotrasmitter release.[47] Therefore, it may be worthwhile exploring the existence of plausible structural and functional parallels between lens fibers and neurons in future studies.[25,48]

Acknowledgments

The authors thank Nikolai Skiba for help with mass spectrometry analysis, Van Bennett (Duke University, Durham, NC, USA) for providing anti–ankyrin-B antibody, and Peter Brophy (Centre for Neuroregeneration, University of Edinburgh, Edinburgh, UK) for providing periaxin-null mice.

Supported by National Institutes of Health Grants R01EY025090 and P30-EY-005722.

Disclosure: **R. Maddala**, None; **P.V. Rao**, None

References

1. Halbleib JM, Nelson WJ. Cadherins in development: cell adhesion, sorting, and tissue morphogenesis. *Genes Dev*. 2006;20:3199–3214.
2. Nishimura T, Takeichi M. Remodeling of the adherens junctions during morphogenesis. *Curr Topics Dev Biol*. 2009;89:33–54.
3. Bassnett S, Shi Y, Vrensen GF. Biological glass: structural determinants of eye lens transparency. *Philos Trans R Soc Lond Ser B Biol Sci*. 2011;366:1250–1264.
4. McAvoy JW, Chamberlain CG, de Iongh RU, Hales AM, Lovicu FJ. Lens development. *Eye*. 1999;13(Pt 3b):425–437.
5. Lovicu FJ, McAvoy JW, de Iongh RU. Understanding the role of growth factors in embryonic development: insights from the lens. *Philos Trans R Soc Lond Ser B Biol Sci*. 2011;366:1204–1218.
6. Cheng C, Nowak RB, Fowler VM. The lens actin filament cytoskeleton: diverse structures for complex functions. *Exp Eye Res*. 2016;156:58–71.
7. Rao PV, Maddala R. The role of the lens actin cytoskeleton in fiber cell elongation and differentiation. *Semin Cell Dev Biol*. 2006;17:698–711.
8. Leonard M, Zhang L, Zhai N, et al. Modulation of N-cadherin junctions and their role as epicenters of differentiation-specific actin regulation in the developing lens. *Dev Biol*. 2011;349:363–377.
9. Leong L, Menko AS, Grunwald GB. Differential expression of N- and B-cadherin during lens development. *Invest Ophthalmol Vis Sci*. 2000;41:3503–3510.
10. Kobielak A, Fuchs E. Alpha-catenin: at the junction of intercellular adhesion and actin dynamics. *Nat Rev Molec Cell Biol*. 2004;5:614–625.
11. Maiden SL, Hardin J. The secret life of alpha-catenin: moonlighting in morphogenesis. *J Cell Biol*. 2011;195:543–552.
12. Leonard M, Chan Y, Menko AS. Identification of a novel intermediate filament-linked N-cadherin/gamma-catenin complex involved in the establishment of the cytoarchitecture of differentiated lens fiber cells. *Dev Biol*. 2008;319:298–308.

13. Walker JL, Zhang L, Menko AS. Transition between proliferation and differentiation for lens epithelial cells is regulated by Src family kinases. *Dev Dynamics*. 2002;224:361–372.
14. Pontoriero GF, Smith AN, Miller LA, Radice GL, West-Mays JA, Lang RA. Co-operative roles for E-cadherin and N-cadherin during lens vesicle separation and lens epithelial cell survival. *Dev Biol*. 2009;326:403–417.
15. Cooper MA, Son AI, Komlos D, Sun Y, Kleiman NJ, Zhou R. Loss of ephrin-A5 function disrupts lens fiber cell packing and leads to cataract. *Proc Natl Acad Sci U S A*. 2008;105:16620–16625.
16. Cain S, Martinez G, Kokkinos MI, et al. Differential requirement for beta-catenin in epithelial and fiber cells during lens development. *Dev Biol*. 2008;321:420–433.
17. Straub BK, Boda J, Kuhn C, et al. A novel cell-cell junction system: the cortex adhaerens mosaic of lens fiber cells. *J Cell Sci*. 2003;116:4985–4995.
18. Rivera C, Yamben IF, Shatadal S, Waldof M, Robinson ML, Griep AE. Cell-autonomous requirements for Dlg-1 for lens epithelial cell structure and fiber cell morphogenesis. *Dev Dynamics*. 2009;238:2292–2308.
19. Takeichi M. Dynamic contacts: rearranging adherens junctions to drive epithelial remodelling. *Nat Rev Molec Cell Biol*. 2014;15:397–410.
20. Leckband DE, de Rooij J. Cadherin adhesion and mechanotransduction. *Annu Rev Cell Dev Biol*. 2014;30:291–315.
21. Barry AK, Tabdili H, Muhamed I, et al. alpha-catenin cytomechanics: role in cadherin-dependent adhesion and mechanotransduction. *J Cell Sci*. 2014;127:1779–1791.
22. Yonemura S, Wada Y, Watanabe T, Nagafuchi A, Shibata M. alpha-Catenin as a tension transducer that induces adherens junction development. *Nat Cell Biol*. 2010;12:533–542.
23. Uchida N, Shimamura K, Miyatani S, et al. Mouse alpha N-catenin: two isoforms, specific expression in the nervous system, and chromosomal localization of the gene. *Dev Biol*. 1994;163:75–85.
24. Mexal S, Berger R, Pearce L, et al. Regulation of a novel alphaN-catenin splice variant in schizophrenic smokers. *Am J Med Genet B Neuropsychiat Genet*. 2008;147B:759–768.
25. Maddala R, Skiba NP, Lalane R III, Sherman DL, Brophy PJ, Rao PV. Periaxin is required for hexagonal geometry and membrane organization of mature lens fibers. *Dev Biol*. 2011;357:179–190.
26. Hirano S, Kimoto N, Shimoyama Y, Hirohashi S, Takeichi M. Identification of a neural alpha-catenin as a key regulator of cadherin function and multicellular organization. *Cell*. 1992;70:293–301.
27. Maddala R, Nagendran T, Lang RA, Morozov A, Rao PV. Rap1 GTPase is required for mouse lens epithelial maintenance and morphogenesis. *Dev Biol*. 2015;406:74–91.
28. Maddala R, Walters M, Brophy PJ, Bennett V, Rao PV. Ankyrin-B directs membrane tethering of periaxin and is required for maintenance of lens fiber cell hexagonal shape and mechanics. *Am J Physiol Cell Physiol*. 2016;310:C115–C126.
29. Bagchi M, Katar M, Lewis J, Maisel H. Associated proteins of lens adherens junction. *J Cell Biochem*. 2002;86:700–703.
30. Meng W, Takeichi M. Adherens junction: molecular architecture and regulation. *Cold Spring Harbor Perspect. Biol*. 2009;1:a002899.
31. Hansen SD, Kwiatkowski AV, Ouyang CY, et al. alphaE-catenin actin-binding domain alters actin filament conformation and regulates binding of nucleation and disassembly factors. *Molec Biol Cell*. 2013;24:3710–3720.
32. Benjamin JM, Kwiatkowski AV, Yang C, et al. AlphaE-catenin regulates actin dynamics independently of cadherin-mediated cell-cell adhesion. *J Cell Biol*. 2010;189:339–352.
33. Rimm DL, Koslov ER, Kebriaei P, Cianci CD, Morrow JS. Alpha 1(E)-catenin is an actin-binding and -bundling protein mediating the attachment of F-actin to the membrane adhesion complex. *Proc Natl Acad Sci U S A*. 1995;92:8813–8817.
34. Abe K, Chisaka O, Van Roy F, Takeichi M. Stability of dendritic spines and synaptic contacts is controlled by alpha N-catenin. *Nat Neurosci*. 2004;7:357–363.
35. Rauskolb C, Sun S, Sun G, Pan Y, Irvine KD. Cytoskeletal tension inhibits Hippo signaling through an Ajuba-Warts complex. *Cell*. 2014;158:143–156.
36. Chopra A, Patel A, Shieh AC, Janmey PA, Kresh JY. alpha-Catenin localization and sarcomere self-organization on N-cadherin adhesive patterns are myocyte contractility driven. *PLoS One*. 2012;7:e47592.
37. Jurado J, de Navascues J, Gorfinkiel N. alpha-Catenin stabilizes cadherin-catenin complexes and modulates actomyosin dynamics to allow pulsatile apical contraction. *J Cell Sci*. 2016;129:4496–4508.
38. Cox-Paulson EA, Walck-Shannon E, Lynch AM, et al. Tropomodulin protects alpha-catenin-dependent junctional-actin networks under stress during epithelial morphogenesis. *Curr Biol*. 2012;22:1500–1505.
39. Gokhin DS, Nowak RB, Kim NE, et al. Tmod1 and CP49 synergize to control the fiber cell geometry, transparency, and mechanical stiffness of the mouse lens. *PLoS One*. 2012;7:e48734.
40. Park C, Falls W, Finger JH, Longo-Guess CM, Ackerman SL. Deletion in Catna2, encoding alpha N-catenin, causes cerebellar and hippocampal lamination defects and impaired startle modulation. *Nat Genet*. 2002;31:279–284.
41. Gillespie CS, Sherman DL, Fleetwood-Walker SM, et al. Peripheral demyelination and neuropathic pain behavior in periaxin-deficient mice. *Neuron*. 2000;26:523–531.
42. Gillespie CS, Sherman DL, Blair GE, Brophy PJ. Periaxin, a novel protein of myelinating Schwann cells with a possible role in axonal ensheathment. *Neuron*. 1994;12:497–508.
43. Grumet M, Mauro V, Burgoon MP, Edelman GM, Cunningham BA. Structure of a new nervous system glycoprotein, Nr-CAM, and its relationship to subgroups of neural cell adhesion molecules. *J Cell Biol*. 1991;113:1399–1412.
44. More MI, Kirsch FP, Rathjen FG. Targeted ablation of NrCAM or ankyrin-B results in disorganized lens fibers leading to cataract formation. *J Cell Biol*. 2001;154:187–196.
45. Bennett V, Lorenzo DN. An adaptable spectrin/ankyrin-based mechanism for long-range organization of plasma membranes in vertebrate tissues. *Curr Top Membr*. 2016;77:143–184.
46. Zhang C, Rasband MN. Cytoskeletal control of axon domain assembly and function. *Curr Opin Neurobiol*. 2016;39:116–121.
47. Joselevitch C, Zenisek D. The cytomatrix protein bassoon contributes to fast transmission at conventional and ribbon synapses. *Neuron*. 2010;68:604–606.
48. Frederikse PH, Kasinathan C, Kleiman NJ. Parallels between neuron and lens fiber cell structure and molecular regulatory networks. *Dev Biol*. 2012;368:255–260.

Investigative Ophthalmology & Visual Science